Thermal characterization of buildings from the monitoring of the AC system consumption

Jorge Payá [a,*], José Miguel Corberán [a], Alvaro de Gracia [b], Albert Castell [c], Luisa F. Cabeza [c]

[a] Instituto de Ingeniería Energética IIE (Universitat Politècnica de València) Camino de Vera s/n, Edificio 8E cubo F 5ª planta, 46022 Valencia, Spain

[b] Center for Advanced Study of Lithium and Industrial Minerals (CELiMIN), University of Antofagasta, Av. Universidad de Antofagasta 02800, Campus Coloso, Antofagasta, Chile

[c] GREA Innovació Concurrent, Universitat de Lleida, Edifici CREA, Pere de Cabrera s/n, 25001, Lleida, Spain

Abstract

This work presents a comparative study between two buildings or cubicles with a same geometry and orientation but with different constructive layers. The mineral wool cubicle is more insulated whereas the alveolar cubicle has more thermal inertia. A novel point in this study has been to evaluate indirectly the thermal load based on the energy consumption of the heat pumps. The results indicate that the mineral wool cubicle consumes up to 7.3% less energy consumption than the alveolar cubicle, particularly in summer. In fact, the load in summer is up to 11.6% higher with the alveolar cubicle, which gains more solar energy during daytime due to its inertia. The power consumption is practically aligned with the outdoor temperatures since it is very sensitive to the operating temperatures. Nevertheless, the peak building load can take place up to 5 hours later than the peak outdoor temperature, particularly in summer and in the alveolar cubicle. Finally, the proposed approach has helped obtained in-situ U-values of 0.20-0.27 W m^{-2} K^{-1} for both cubicles.

Keywords: buildings, energy consumption, heat pumps, experimental, modelling

**Corresponding author*. Tel: +34 963879910; Fax: +34 963877272;

E-mail address: jorpaher@iie.upv.es (J. Payá)

NOMENCLATURE

COP	Coefficient of Performance	EER	Energy Efficiency Ratio
f	Compressor frequency (Hz)		
$\dot{W}$	Power consumption (W)	$\dot{Q}$	Thermal power (W)
W	Energy consumption (Wh)	Q	Thermal capacity (Wh)
C	Fitted parameter in Eq. (1)	t	Time (s)
K	Fitted parameter in Eq. (2)	A	Internal wall area (m^2)
$Q_{building}$	Effective load of the building eliminating the effect of the inverter and fans	β	Weight of residual energy consumption in the total energy consumption (%)
$\overline{I_{solar}}$	Mean solar irradiance on the entire cubicle (W)	UA	Overall heat transfer coefficient (W/K)
R	Thermal resistance ($K\ W^{-1}$)	e	Thickness (m)
h	Convective heat transfer coefficient ($W\ m^{-2}\ K^{-1}$)	D_{on}	Duration of period (%)when the compressor is ON
k	Thermal conductivity ($W\ m^{-1}\ K^{-1}$)	α	Thermal diffusivity ($m^2\ s^{-1}$)
Subscripts			
h	Heating mode	c	Cooling mode
out	Outdoor	in	Indoor
std	Standard EUROVENT conditions	nom	Nominal operation point
on	Compressor ON	off	Compressor OFF
res	Residual consumption of the heat pump	ratio	EER, $\dot{Q}$ or $\dot{W}$ referred dimensionless to standard temperature conditions
campaign	Mean value of parameters during the entire experimental campaign	exp	Experimental
side	Lateral walls of the cubicles	top	Top of the cubicles
ALV	Alveolar cubicle	MW	Mineral wool cubicle
Min	Minimum	Max	Maximum

1. INTRODUCTION

Energy consumption is growing worldwide and one of the major consumers is the building sector [1]. In order to mitigate this impact, the European Directive 2010/31/EU [2] states that by 2020 new buildings must consume “nearly zero” energy and reduce the global energy consumption and greenhouse gases emissions down to 20% before 2020.

Different approaches are being applied to reach such objectives. Passive strategies aim to reduce the energy demand, such as by improving the thermal insulation ([3][4]) or increasing the thermal inertia ([5]7]) of the building envelopes. N. Aste et al. (]8]) recently analyzed the impact of external wall systems with the same thermal transmittance (U-value) but with different thermal inertia. Some attempts have been done to combine thermal insulation and inertia, demonstrating that significant energy savings can be achieved [6]. The distribution of thermal inertia and insulation within the wall has also been studied [9], demonstrating that distributed insulation and inertia is the best option. Simulation studies based on multiobjective algorithms have helped to select the wall layers disposition [10-12]. Very recently, a full assessment of cost-optimality and technical solutions has been carried out by I. Zacà et al. ([13]) for multi-residential buildings in the Mediterranean region.

Regarding active systems a significant attention has been attracted on renewables and highly efficient technologies, for instance solar energy. However, heat pumps are considered as an already stablished technology that can achieve high energy savings. In fact, they are included in the Directive on the promotion of the use of energy from renewable sources (209/28/EC) as an environmentally friendly technology 0 which can help reduce the CO_2 emissions 0. Recent trends, for instance in heat pump systems for residential applications consist in using scroll compressors with variable compressor speeds [16] which can help to achieve further energy savings.

When comparing the performance of existing buildings, a key point is to evaluate their thermal load and the U-value in steady state. The thermal load can be evaluated via many software tools [17], but this approach presents several drawbacks. For instance, a major source of uncertainty in simulations is the inaccuracy in the estimation of the thermal resistance or the thermal mass of the different wall layers [18-19]. Further uncertainties reside in unavoidable construction defaults leading to thermal bridges,

contact thermal resistances, gaps in materials, air movement in cavities and infiltrations [20-23].

Many of the previous uncertainties can be eluded by using in-situ measurements [20-21, 24]. Such techniques generally require the monitoring of heat fluxes and indoor/outdoor temperatures in walls with different constructive layers and in practice they are hard to obtain.

This paper presents a simplified in-situ approach for the thermal characterization of existing buildings from the monitoring of the air-conditioning system consumption. The described method presents a series of advantages. Firstly, it enables the characterization of the heat pump behavior under dynamic working conditions and to detect potential failures. Secondly, when applied to buildings with different constructive layers and thermal zones, it requires a minimum of monitoring equipment, basically the indoor and outdoor temperatures as well as the Air-Conditioning Heat Pump (AC-HP) energy consumption. Finally, the developed approach helps to calculate the U-value, the thermal delay between the load and outdoor temperatures as well as relevant performance indicators such as the EER or COP of the AC-HP. Although the performance of the heat pump is reproduced via performance maps, as usual in the field [25], a simplified approach is proposed to evaluate the operating frequency.

2. MATERIALS AND METHODS

2.1 Experimental set-up

A set-up consisting of several house-like constructions (named cubicles from here onwards), with internal dimensions of 2.4 x 2.4 x 2.4 m, was built and is located in Lleida (Spain). In this work, two different constructive systems are compared. A heat pump has provided the required heating or cooling to the cubicles in order to keep a desired indoor constant temperature. The consequent energy consumption has been measured for different tests under real weather conditions. The main differences between the two tested cubicles are the thermal resistance and the thermal inertia of the walls, since one is based on the thermal insulation concept and the other one on the use of thermal mass in the envelope.

2.1.1 Insulated cubicle

The mineral wool cubicle (MW) was built with a double brick constructive system. Four structural pillars of reinforces concrete are located at each corner. The walls are composed of an internal perforated brick (29 x 14 x 7.5 cm), an air chamber of 5 cm, 5 cm of mineral wool as insulation and an external layer of hollow brick (50 cm x 20 cm x 7.5 cm). The internal and external finishing are gypsum and mortar, respectively (Figure 1). The roof was constructed using concrete precast beams and 5 cm of concrete slab. The insulating material is placed over the concrete, protected with a cement mortar roof with an inclination of 3% and a double asphalt membrane. More details on the MW cubicle can be found in [3] and [26]. The thermo-physical properties of the different layers are summarized in Table 1.

	e (cm)	ρ (kg m^{-3})	k (W m^{-1} K^{-1})	α (m^2 s^{-1})	Order in ALV-roof	Order in ALV-sides	Order in MW-roof	Order in MW-sides
Cement mortar	1	1350	0.7	5.18E-07	3	2 (out)	3	6 (out)
Hollow brick	7	930	0.375	4.03E-07	-	-	-	5
Polyurethane	5	35	0.028	8.00E-07	2	-	-	-
Mineral wool	5	100	0.035	3.50E-07	-	-	2	3
Perforated brick	14	900	0.543	6.03E-07	-	-	-	2
Concrete beam	25	760	0.472	6.21E-07	1 (in)	-	1 (in)	-
Asphalt membrane	1	2100	0.7	3.30E-07	4 (out)	-	4 (out)	-
Alveolar brick	29	1080	0.27	5.19E-07	-	1 (in)	-	-
Gypsum	1	1150	0.57	4.96E-07	-	-	-	1 (in)
Air chamber	5	-	-	-	-	-	-	4

Table 1. Thermo-physical properties of the different wall layers

2.1.2 Thermal mass cubicle

The alveolar brick cubicle (ALV) has bricks of 30 x 19 x 29 cm and an internal and external finishing of gypsum and mortar, respectively (Figure 1). The alveolar brick has a special design which provides both thermal and acoustic insulation [26]. No structure was necessary and no additional insulation was used in the walls. The roof system is the same in the two tested cubicles except for the insulation material which is either

mineral wool (MW cubicle) or polyurethane (ALV cubicle). The thermo-physical properties of the different wall layers are given in Table 1.

Figure 1. Cubicles of the experimental campaign. Insulated cubicle (MW, left) and inertial cubicle (ALV, right).

2.1.3 Instrumentation and monitoring

In order to monitor and analyse the performance of the different constructive systems the following data were registered at five minutes interval:

- Weather conditions (solar radiation (Middleton Solar pyranometers SK08) with an accuracy of ±5%, ambient temperature and humidity (ELEKTRONIK EE21) with an accuracy of ±2%, wind velocity (DNA 024 anemometer)).
- Internal ambient temperature (ELEKTRONIK EE21) with an accuracy of ±2%.
- Internal surface temperature of the walls, roof and ceiling (Pt-100 DIN B, calibrated with a maximum error of ±0.3ºC).
- External surface temperature of the south wall (Pt-100 DIN B, calibrated with a maximum error of ±0.3ºC).
- Energy consumption of the heating/cooling systems with an electrical network analyser (MK-30-LCD).

2.2 Experimental procedure

The experimental campaign involved both summer and winter conditions. The heat pump was set to a constant indoor temperature and either heating or cooling was provided depending on the season. Different set-point temperatures were tested under

real outdoor conditions. Side by side experiments were performed in both cubicles; therefore, the same temperature set-points were tested.

Table 2 presents the different experiments which have been performed. A same indoor set-point temperature of 18ºC has been applied both in winter and summer for a better comparison of the results.

Mode	Campaign	Indoor Set-point	Week
Heating	H21	21ºC	Last week December 2012
	H18	18ºC	2-3rd week January 2013
Cooling	C24	24ºC	1-2nd week July 2012
	C18	18ºC	3-4th week July 2012

Table 2. Experimental campaign

2.3 Modelling approach

The heat pump installed in each cubicle is the model ASHA07LCC from FUJITSU GENERAL, an inverter, reversible class A heat pump with R410A as refrigerant. The performance specifications given by the manufacturer are summarized in Table 3. One aspect to be emphasized is that the manufacturer only provides a performance range for the thermal power, whereas the power consumption or the efficiency indicators (Energy Efficiency Ratio EER in cooling mode or Coefficient of Performance COP in heating mode) are only given for the nominal point of the heat pump. The latter corresponds to a frequency of 60 Hz under EUROVENT temperatures (T_{out}^{std}=35ºC, T_{in}^{std}=27ºC for cooling; T_{out}^{std}=7ºC, T_{in}^{std}=20ºC for heating).

Figure 2 shows a scheme of the modelling approach which has been followed starting in step 1 with the previous collection of data from the manufacturer. Real operation conditions are completely dynamic with variable indoor/outdoor temperatures and variable compressor speeds. Thus, in step 2 a wider set of operation points has been created based on typical performance data of air-to-air heat pumps. The linear fitting

of the capacity (Figure 2) and the power consumption (Figure 3) ensures that the predicted performance is in agreement with the manufacturer data (Table 3).

Mode	Feature (units)	Value
Cooling	Thermal power (W)	2100 (500-3000)
	Power consumption (W)	470
	EER	4.47
Heating	Thermal power (W)	3000 (500-4600)
	Power consumption (W)	840
	COP	4.55

Table 3. Manufacturer performance data of the heat pumps

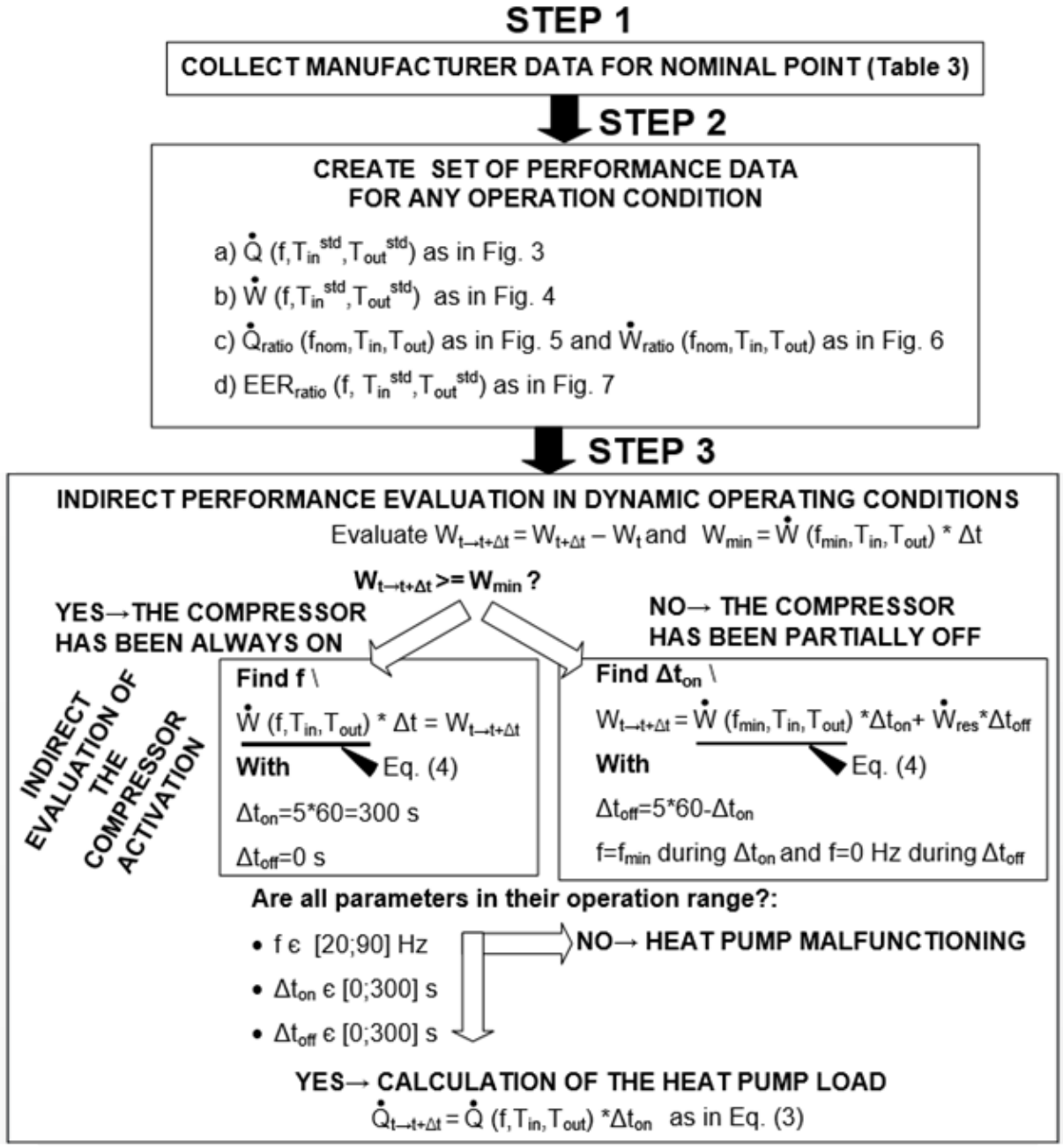

Figure 2. Calculation scheme to evaluate the AC-HP performance

The manufacturer provides a range of capacities (Table 3) and hence these are a good estimation of the performance for the operation frequencies of 20 Hz (minimum), 60 Hz (nominal point) and 90 Hz (maximum). In step 2a) the capacities provided by the manufacturer (Table 3) have been correlated with the operating frequency (Figure 3). A linear interpolation provides accurate correlations given the high R^2 values (R^2>0.99).

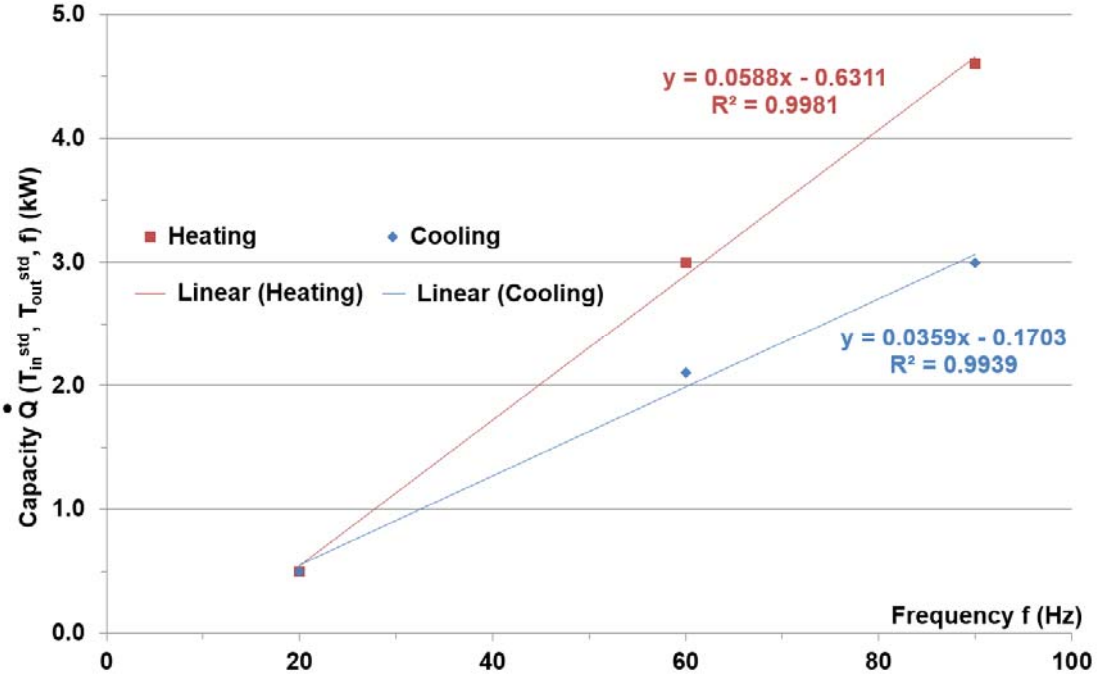

Figure 3. Capacity vs frequency of the heat pump

In step 2b), the power consumption has been assumed to be linear with the operating frequency, hereby providing the correlations given in Figure 4.

In step 2c), the performance has been supposed to vary with the indoor and outdoor temperature as for typical heat pumps characterized in the Ecodesign Directive [27]. This approach has led to the capacity and power consumption curves represented in Figures 5 and 6 for the cooling mode. The developed correlations for both heating and cooling respond to Eqs. (1-2) and the full parameters are listed in Table 4.

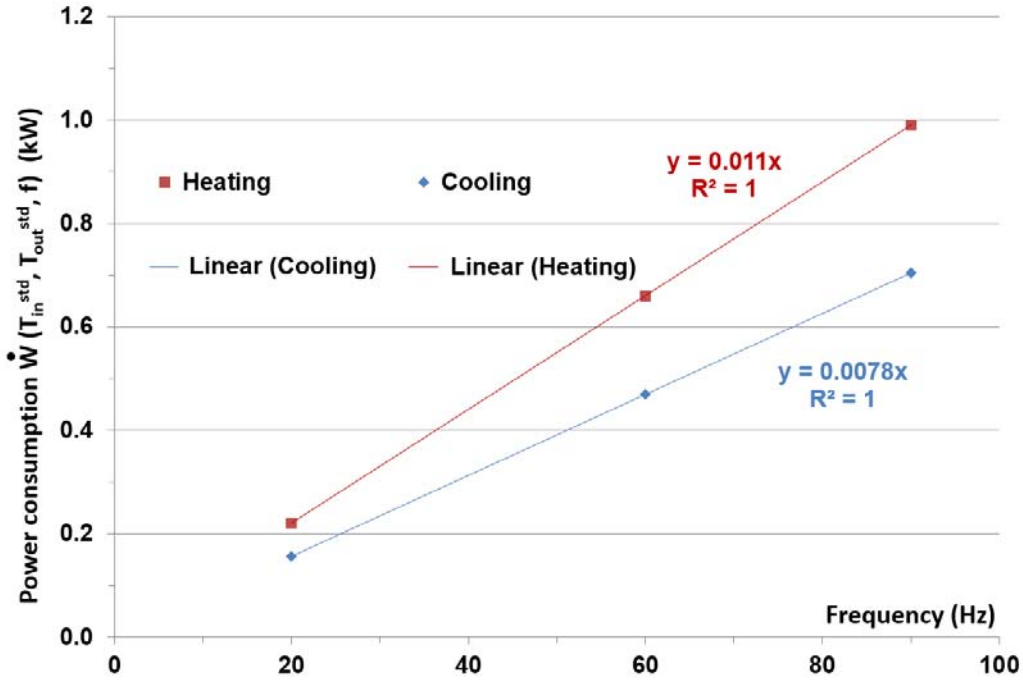

Figure 4. Power consumption vs frequency of the heat pump

$$\dot{Q}_{ratio}(T_{in};T_{out}) = \frac{\dot{Q}\,(T_{in};T_{out};f_{nom})}{\dot{Q}\,(T_{in}^{std};T_{out}^{std};f_{nom})} = 1 + C_1 \cdot \left(T_{in} - T_{in}^{std}\right) + C_2 \cdot \left(T_{out} - T_{out}^{std}\right) + C_3 \cdot \left(T_{in} - T_{in}^{std}\right)^2 + C_4 \cdot (T_{out} - T_{out}^{std})^2 \quad (1)$$

$$\dot{W}_{ratio}(T_{in};T_{out}) = \frac{\dot{W}\,(T_{in};T_{out};f_{nom})}{\dot{W}\,(T_{in}^{std};T_{out}^{std};f_{nom})} = 1 + K_1 \cdot \left(T_{in} - T_{in}^{std}\right) + K_2 \cdot \left(T_{out} - T_{out}^{std}\right) + K_3 \cdot \left(T_{in} - T_{in}^{std}\right)^2 + K_4 \cdot (T_{out} - T_{out}^{std})^2 \quad (2)$$

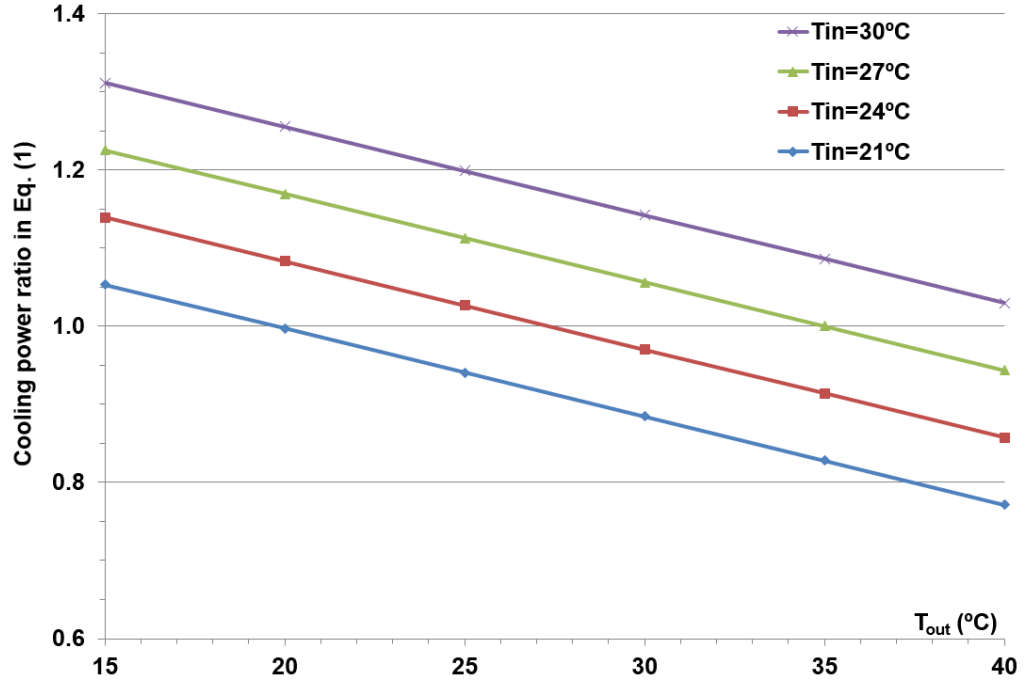

Figure 5. Cooling thermal power ratio vs outdoor temperature (Eq. (1))

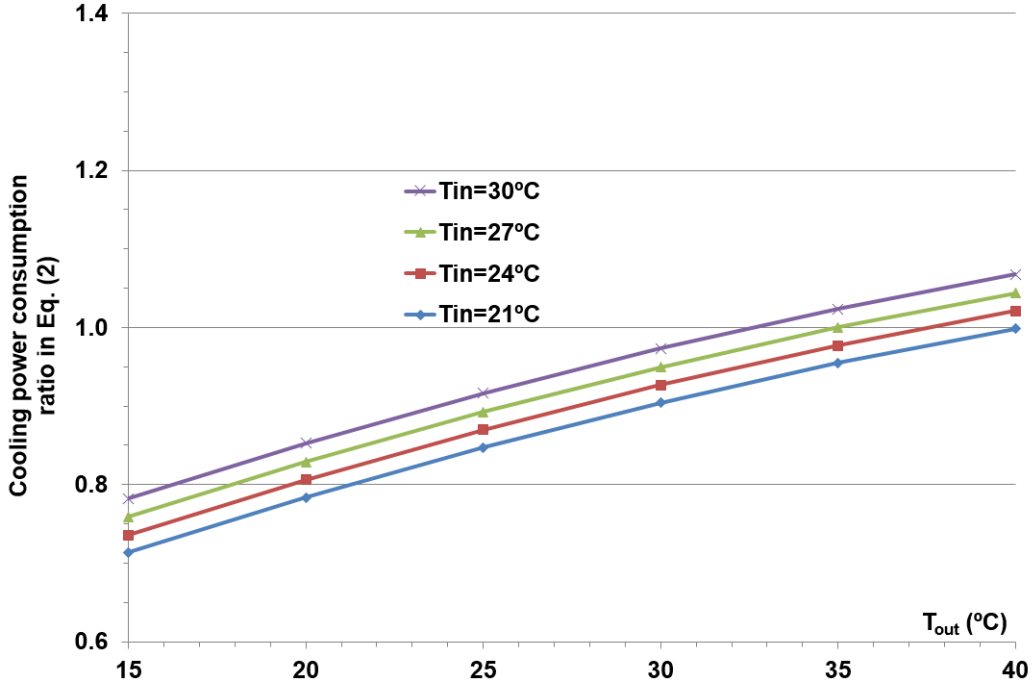

Figure 6. Cooling power consumption ratio vs outdoor temperature (Eq. (2))

Parameter	Cooling	Heating
$\dot{Q}_{nom}$ (W)	2100	3000
$\dot{W}_{nom}$ (W)	470	660
$\dot{W}_{res}$ (W)	11.8	12
C_1	2.868 E-02	2.373 E-02
C_2	-1.128 E-02	-2.771 E-03
C_3	-1.541 E-06	1.618 E-04
C_4	-3.534 E-07	-3.861 E-05
K_1	7.764 E-03	8.484 E-03
K_2	9.423 E-03	9.154 E-03
K_3	3.791 E-05	1.225 E-05
K_4	-1.317 E-04	6.907 E-05

Table 4. Parameters of the heat pump correlations

The total energy consumption of the heat pump including the compressor and fans is measured with a recording interval of 5 minutes. Given that the indoor and outdoor temperatures are also measured, step 3 consists in predicting how the compressor has worked during this time interval. Firstly, it is necessary to determine if the compressor has been on the full time and to know which was the operating frequency. Knowing this, on a final stage it is possible to evaluate the thermal load. Using the scheme illustrated in Figure 2, if the measured energy consumption is less than the consumption required at 20Hz, then the compressor has been partially off. For every recording interval of 5 minutes, one value is fitted, either the operation frequency if the compressor is always on, or the duration of the on-period when the compressor has been partially off. Finally, the load and power consumption are evaluated using Eqs. 3 to 5.

$$\dot{Q} = \dot{Q}(f) \cdot \dot{Q}_{ratio}(T_{in}; T_{out}) \tag{3}$$

$$\dot{W} = \frac{\dot{Q}(f)}{EER(f)} \cdot \dot{W}_{ratio}(T_{in}; T_{out}) \tag{4}$$

$$EER(f) = EER_{ratio}\left(\frac{f}{fmax}\right) \cdot EER_{fmax} = EER_{ratio}\left(\frac{f}{fmax}\right) \cdot \frac{EER_{nom}}{1.2} \tag{5}$$

Eq. (5) has been obtained from recent literature on typical air to air heat pumps [21]. The polynomial correlation EER_{ratio} (f/f_{max}) shown in Figure 7 has been obtained using the data of published literature [27].

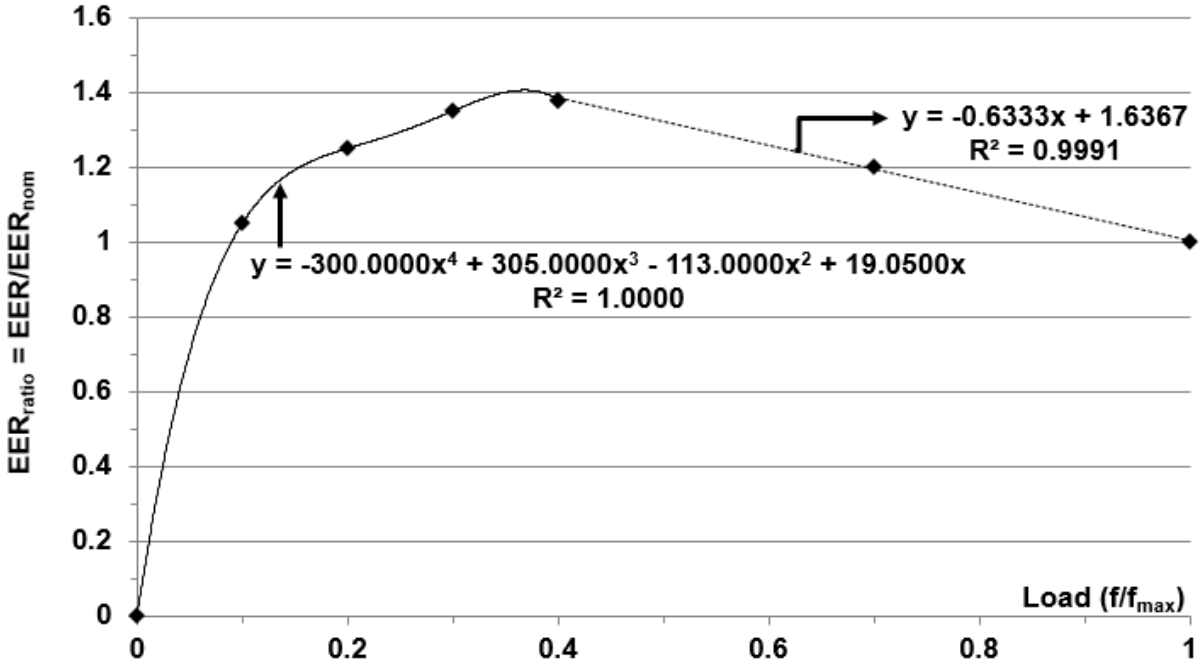

Figure 7. EER ratio vs load (f/f_{max})

3. RESULTS AND DISCUSSION

The monitoring data have been analysed and summarized as shown in Table 5. According to the mean power consumption of the campaign, the MW cubicle seems to consume less for same indoor & outdoor conditions. In winter the power consumption is reduced by 0.9% (test H18) and 1.6% (test H21). In summer the differences are noticeable, 2.7% less in test C18 and 7.3% less in test C24. However, in order to conclude anything regarding the thermal loads it is first necessary to understand how the heat pumps have performed in each cubicle.

Test	C18		C24		H21		H18	
Cubicle	**ALV**	**MW**	**ALV**	**MW**	**ALV**	**MW**	**ALV**	**MW**
$T_{in,min}$ (ºC)	16.1	16.2	23.0	23.1	19.0	19.5	18	18.5
$\overline{T_{in}}$ (ºC)	16.8	16.9	23.6	24.0	22.0	22.4	18.9	19.4
$T_{in,max}$ (ºC)	17.4	17.5	24.1	24.5	22.9	23.2	19.5	20.9
$T_{out,min}$ (ºC)	12.8	12.8	15.2	15.2	-4.3	-4.3	-5.1	-5.1
$\overline{T_{out}}$ (ºC)	24.8	24.8	24.4	24.4	4.6	4.6	7.0	7.0
$T_{out,max}$ (ºC)	37.7	37.7	34.0	34.0	15.3	15.3	15.1	15.1
$\overline{T_{out}} - \overline{T_{in}}$ (ºC)	8.0	7.9	0.9	0.5	-17.5	-17.9	-11.9	-12.4
$\overline{I_{solar}}$ (W)	1236	1236	1163	1163	417	417	419	419
$\overline{W}$ (kW)	0.1649	0.1604	0.0591	0.0548	0.2604	0.2563	0.1962	0.1945

Table 5. Summary of direct monitoring data

Figure 8 represents the hourly building load in summer, as evaluated using the previous modelling approach. The building load has been calculated by eliminating the effect of the residual power consumption (12W) and the fans (60W) which in the entire experimental campaign tend to decrease (winter) or increase (summer) the load which has to be covered by the AC-HP.

The peak thermal load in both cubicles is delayed with respect to the maximum ambient temperature by around 3-5h. The maximum ambient or outdoor temperature was of 37.7ºC on the 19/07/2012. The ALV cubicle, with more thermal inertia, generally has its peak thermal load around 1-3h later than the MW cubicle. The main difference between both cubicles is that the ALV cubicle gains more solar energy during daytime, and this heat is released inside the cubicle in the afternoon, hereby increasing its load with respect to the MW cubicle. However, the higher thermal lag provided from the ALV cubicle might make free cooling ventilation strategies possible in order to dissipate this higher solar gains.

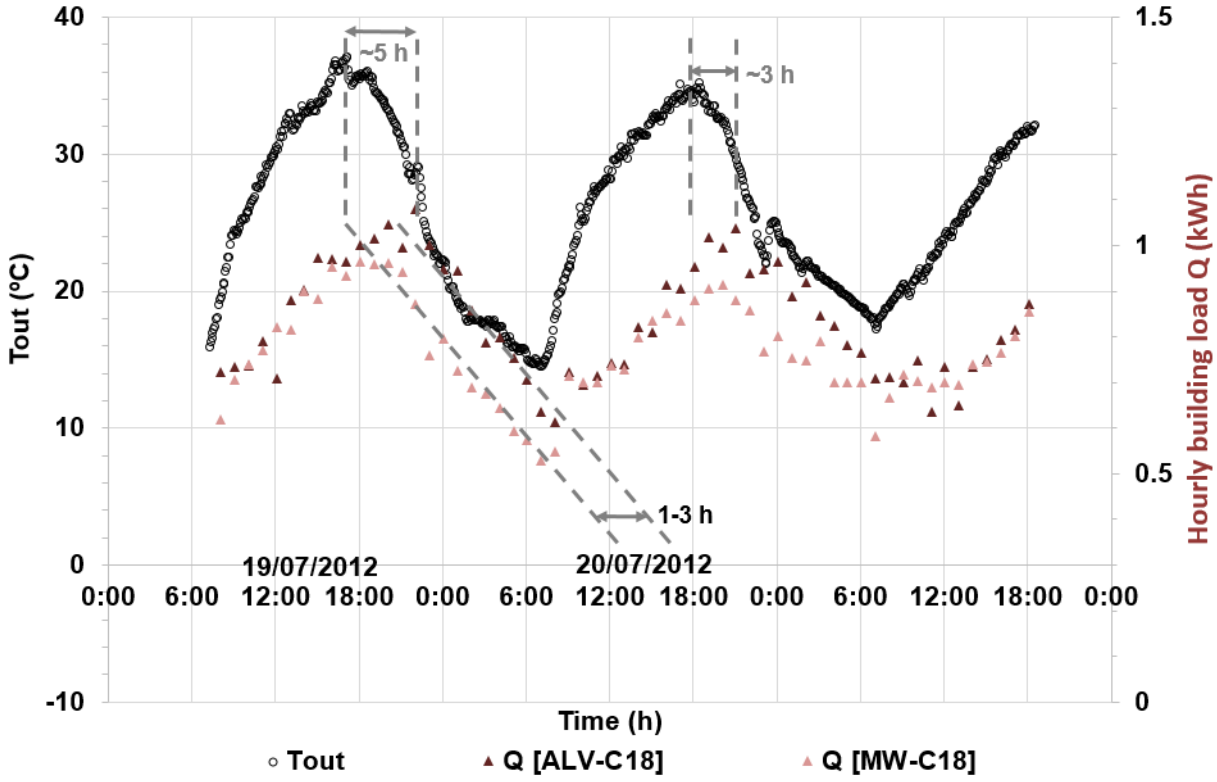

Figure 8. Hourly building load in summer for both cubicles

Figure 9 represents the hourly energy consumption of the heat pumps. The MW energy consumption is practically synchronised with the outdoor temperature, whereas the ALV cubicle energy consumption presents a delay of 1-2 hours depending on the day. This short delay with respect to the outdoor temperatures is due to the fact that the power consumption depends significantly on the outdoor temperature (Figure 6). In the afternoon, even if the thermal loads are higher (Figure 8), the outdoor temperatures drop and consequently the heat pumps work with a better EER and the power consumption decreases. Given the additional solar energy gain, the heat pump energy consumption is generally higher in the ALV cubicle from 17:00 to 07:00.

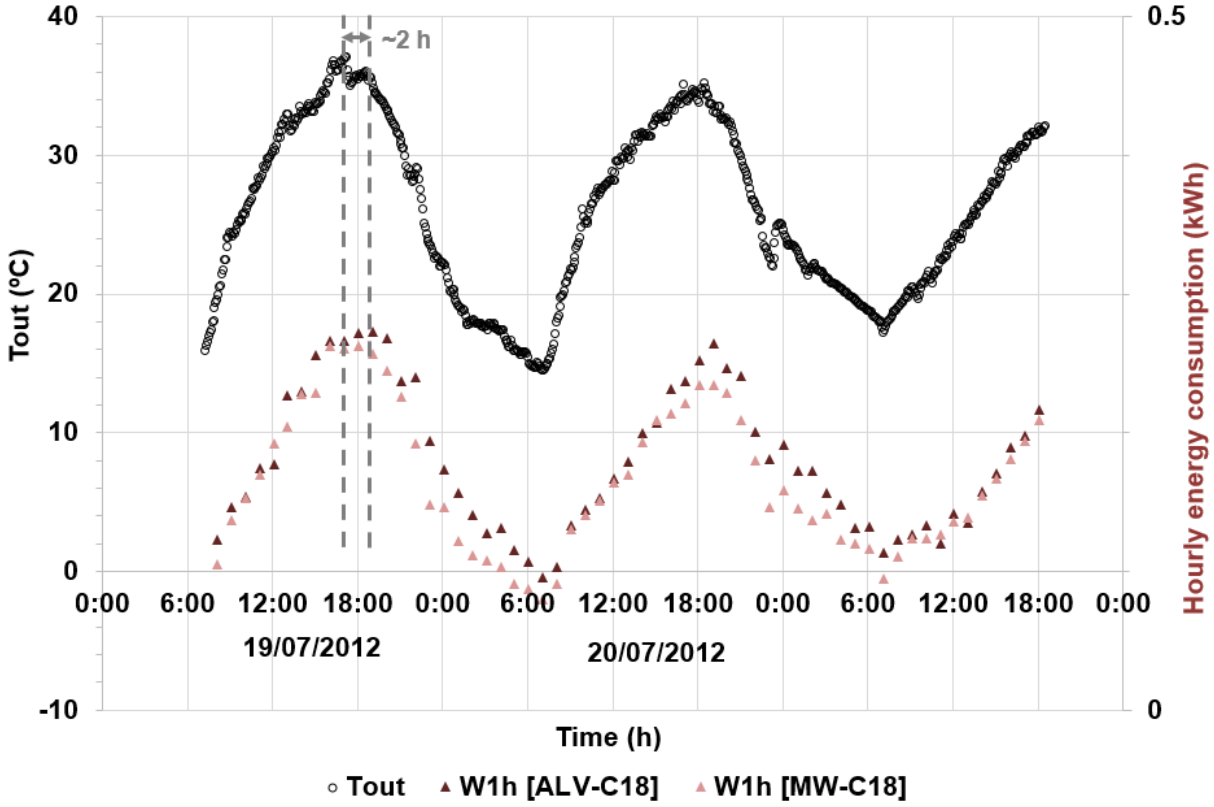

Figure 9. Hourly energy consumption in summer for both cubicles

In winter conditions, the hourly thermal load and the energy consumption of the heat pumps present the tendencies shown in Figures 10 and 11. The first day has a particularly low outdoor temperature at night (down to -5.1ºC) and consequently the inter-daily load variation is higher than on the second day, where the minimum outdoor temperature just dropped down to 4.6ºC. As occurs for summer conditions, the energy consumption is almost synchronised with the outdoor temperature. The differences between both cubicles in terms of thermal load or energy consumption are rather small, as could also be inferred from the analysis of Table 5. The peak thermal load takes place around two hours later than the minimum outdoor temperature. In winter, given that the solar energy gain is smaller than in summer, both cubicles present a similar performance which is mainly driven by the difference between the indoor and outdoor temperatures. As explained before, in summer transient effects due to the solar energy gain in the walls become significant in addition to the indoor and outdoor temperature difference.

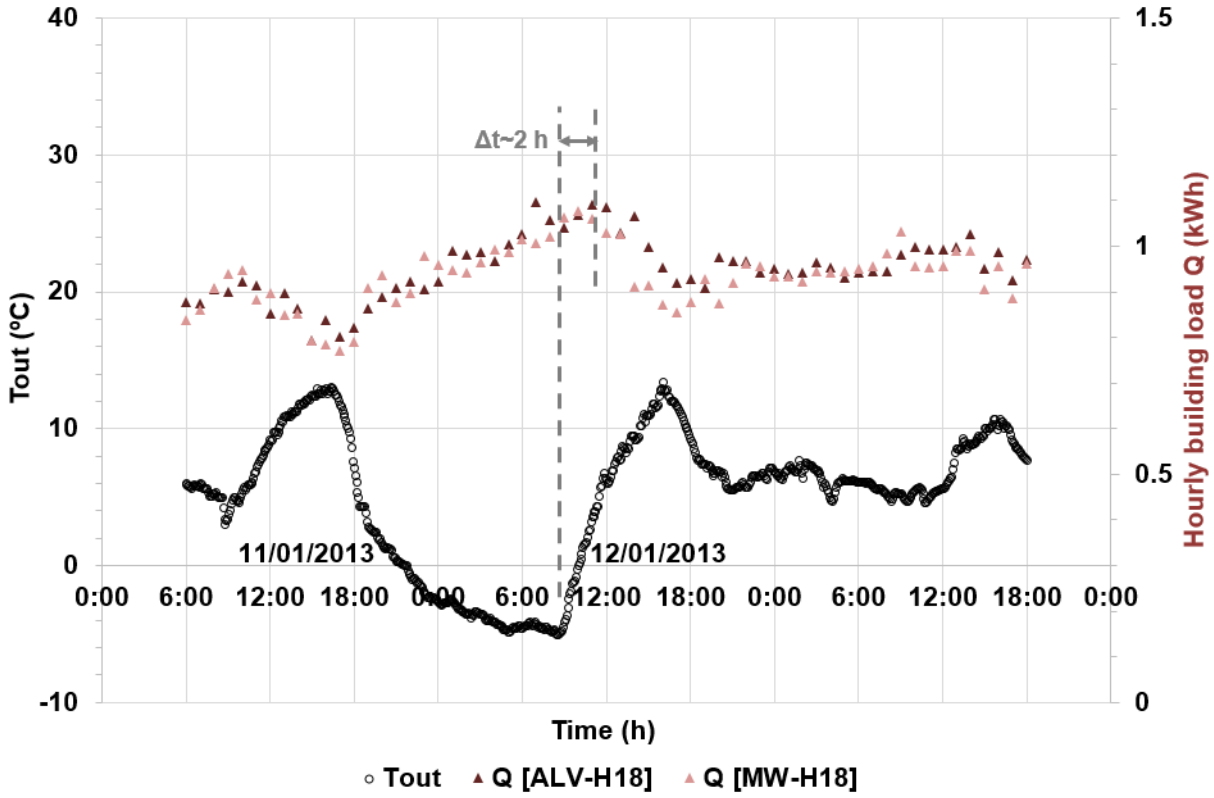

Figure 10. Hourly building load in winter for both cubicles

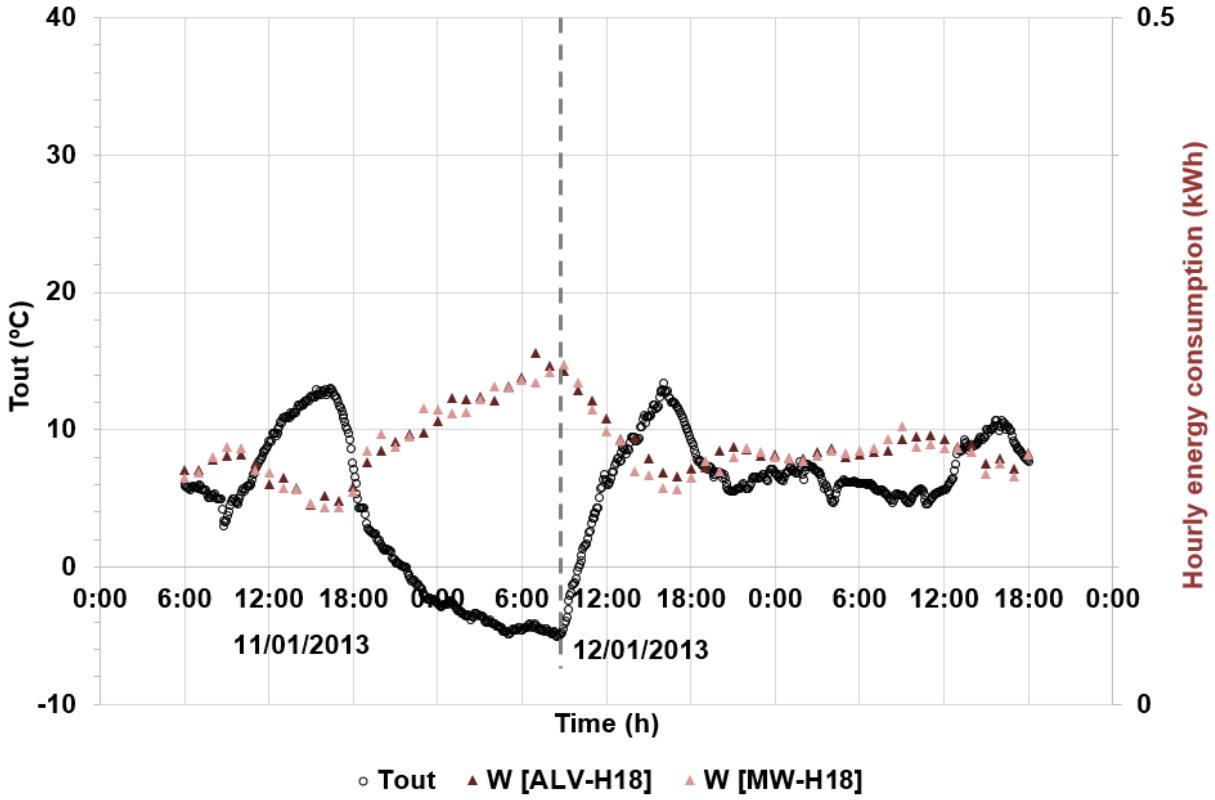

Figure 11. Hourly energy consumption in winter for both cubicles

Table 6 presents a summary of the heat pump performance in both cubicles, as obtained by applying the previous modelling approach.

From the point of view of the global system performance, the building load is always smaller in the case of the MW cubicle. In winter the thermal load is only decreased by 1.5% (H18) and 1.6% (H21). In summer the differences are noticeable, and the thermal load is decreased in the MW cubicle by 4.2% (C18) and 11.6% (C24). As explained before, the ALV cubicle has a higher load, particularly in the evening when the warm walls heat up the cubicles due to the solar radiation they have absorbed during daytime.

As expected, the higher the set-point requirements, the higher the load and energy consumption in both heating and cooling. The overall EER or COP of each experimental campaign is in the range from 4.8 to 5.2. In general terms, the higher the set-point requirements, the lower the EER or COP. The mean operating frequency of the heat pumps is in the range from 24 to 36 Hz, hereby indicating that the heat pumps face a relatively small load with respect to their maximum capacity.

The compressor is generally on during all the experimentation, except for the cooling test C24, where it is only ON around D_{on} = 40% of the experimental campaign. In such test, the residual power consumption of the heat pump accounts for β =12-13%, whereas in the rest of the tests its contribution is rather small.

Test		C18		C24		H21		H18	
Cubicle		ALV	MW	ALV	MW	ALV	MW	ALV	MW
GLOBAL SYSTEM PERFORMANCE	$\overline{Q}_{building}$ (kW)	0.730	0.699	0.267	0.236	1.318	1.297	1.088	1.072
	$\overline{Q}_{AC-HP}$ (kW)	0.795	0.766	0.298	0.266	1.246	1.225	1.016	1.001
	EER / COP	4.8	4.8	5.0	4.8	4.8	4.8	5.2	5.1
	$\overline{f}$ (Hz)	36	33	25	24	34	33	28	28
	D_{on}	0.88	0.92	0.40	0.39	1.00	1.00	0.99	0.99
	β	0.01	0.01	0.12	0.13	0.00	0.00	0.00	0.00
	U_{exp} (W K^{-1})	0.27	0.26	0.20	0.21	0.21	0.20	0.25	0.23
PERFORMANCE DURING ON-PERIODS	$\overline{Q}_{on}$ (kW)	0.902	0.835	0.743	0.690	1.246	1.225	1.027	1.011
	EER_{on}	4.9	4.8	5.8	5.6	4.8	4.8	5.2	5.2
	$\overline{W}_{on}$ (kW)	0.185	0.174	0.129	0.123	0.260	0.256	0.198	0.196

Table 6. Summary of the heat pump performance in both cubicles

By means of the developed approach, the EER or COP can be evaluated both for the entire experimental campaign and when the heat pump is exclusively on. This is particularly interesting for the experimental campaign C24, where the compressor is only on around 40% of the experimentation. In C24, the overall EER of the campaign is 5.0 (ALV) and 4.8 (MW). However, regarding only when the compressor is on, the EER is 5.8 (ALV) and 5.6 (MW). Consequently, when the heat pump is on, the favourable set-point temperatures allow for a high EER_{on}, although from the point of view of the entire campaign, the overall EER is lower and comparable to C18, because 60% of the experimentation takes place with the compressor off, with no cooling production but with a residual power consumption.

The calculated EER or COP are relatively high because the proposed approach assumes that the heat pumps are working following their performance map.

Consequently, these parameters should be taken mainly as a criterion to compare both cubicles rather than by their absolute value.

Eq. (6) shows the in-situ estimation of the thermal transmittance or U-value of the cubicles. The U-value depends on the characteristics of the different constructive layers which are detailed in recent literature [26]. Given that the wall layers in the lateral walls and the roof are different, two thermal resistivities (R_{sides} and R_{top}) have been placed in parallel. The theoretical U-value of the entire cubicle is only an indicator of the heat transfer with the ambient given that the cubicles are never really in stationary conditions, and that the thermal inertia of the walls, particularly relevant in the case of the ALV cubicle, are not considered in the equations.If the buildings were in stationary conditions, the thermal load would be directly proportional to the U-value and to the difference between the indoor and outdoor temperatures.

$$U_{exp} = \frac{\int_0^t \dot{Q}.dt}{\int_0^t (T_{in} - T_{out}).dt} \cdot \frac{1}{A} = \frac{\sum_j Q_{5min,j}}{\sum_j |T_{in,j} - T_{out,j}|} \cdot \frac{1}{A} \quad (6)$$

$$U = \frac{R_{sides} + R_{top}}{R_{sides} \cdot R_{top}} \quad (7)$$

$$R = \frac{1}{h_{in}} + \sum \frac{e_i}{k_i} + \frac{1}{h_{top,out}} \quad (8)$$

The experimental U-value is in the range 0.20-0.27 W m^{-2} K^{-1} for both cubicles. According to the theoretical calculation, U_{MW} ~ 0.41 W m^{-2} K^{-1} < U_{ALV} ~ 0.71 W m^{-2} K^{-1}. This difference is in coherence with published literature [24, 26] which indicates that theoretical calculations of U-values tend to overestimate the in-situ values. The experimental values are closer to the theoretical calculation in the case of the MW cubicle given that it has a small thermal inertia. The ALV cubicle has a significant inertia and this is not addressed in the theoretical calculation. As the experimental U-values are very close in both cubicles, this implies in a certain sense that the inertia of the ALV cubicle compensates the lack of insulation. Similar conclusions were provided by de Gracia et al. [26] who highlighted the necessity of evaluating the transient performance of the different constructive systems in the design phase of new and refurbished buildings.

4. CONCLUSIONS

This article presents an experimental and theoretical analysis of two cubicles with different constructive designs, but with same heat pumps and same indoor/outdoor conditions.

The alveolar cubicle has more thermal inertia and less insulation. The mineral wool cubicle consumes up to 1.6% less power consumption in winter and up to 7.3% less in summer. By means of the developed approach, it is possible to deduce how the heat pumps have performed and to obtain both the thermal load and detailed operating parameters such as the frequency, the on/off periods and the EER or COP.

In winter, the thermal load with the mineral wool cubicle is decreased by up to 1.6% (H21). However, in summer the differences are more noticeable, and the thermal load can be decreased up to 11.6% (C24). In fact, the higher the thermal inertia of the walls (alveolar cubicle), the higher the solar gain and the heat pump has to face more thermal load, generally from 17:00 to 07:00.

The heat pump performance is very sensitive to the operating temperatures and consequently the energy consumption is practically synchronised with the outdoor temperatures, especially in the mineral wool cubicle. However, the building load can present a delay of up to 5 hours with respect to the outdoor temperatures, particularly in the alveolar cubicle and in summer due to the additional solar energy gain.

The developed approach has helped to conclude that both heat pumps are working properly, with no failures, and with high overall COPs/EERs (4.8-5.2). Moreover, in some specific cases, such as test C24 with very low power requirements, the compressor is only on 40% of the campaign, and even if the EER is particularly high when the compressor is on (5.6-5.8) the overall EER of the campaign drops down to (4.8-5.0) given the long off-periods when the heat pump presents a residual power consumption and does not remove any heat load. Finally, the proposed approach has helped obtain experimental U-values in the range 0.20-0.27 W m^{-2} K^{-1} for both cubicles.

ACKNOWLEDGEMENTS

The work partially funded by the Spanish government (ULLE10-4E-1305). The authors from Lleida would like to thank the Catalan Government for the quality accreditation given to their research group (2014 SGR 123). The research leading to these results has received funding from the European Union's Seventh Framework Programme (FP7/2007-2013) under grant agreement No. PIRSES-GA-2013-610692 (INNOSTORAGE). This project has received funding from the European Union's Horizon 2020 research and innovation programme under grant agreement No. 657466 (INPATH-TES). Alvaro de Gracia would like to thank the Education Ministry of Chile for Grant PMI ANT1201.

REFERENCES

[1] International Energy Agency. Energy Technology Perspectives 2012. Pathways to a clean energy system. International Energy Agency 2012, Paris.

[2] Directive 2010/31/EU of the European parliament and of the council of 19 May 2010 on the energy performance of buildings. Available from: http://www.epbd-ca.eu (accessed November 2015).

[3] L.F. Cabeza, A. Castell, M. Medrano, I. Martorell, G. Pérez, I. Fernández. Experimental study on the performance of insulation materials in Mediterranean construction. Energy and Buildings 42 (2010) 630–636.

[4] I. Axaopoulos, P. Axaopoulos, J. Gelegenis. Optimum insulation thickness for external walls on different orientations considering the speed and direction of the wind. Applied Energy 117 (2014) 167–175.

[5] A. Gagliano, F. Patania, F. Nocera, C. Signorello. Assessment of the dynamic thermal performance of massive buildings. Energy and Buildings 72 (2014) 361–370.

[6] N. Aste, A. Angelotti, M. Buzzetti. The influence of the external walls thermal inertia on the energy performance of well insulated buildings. Energy and Buildings 41 (2009) 1181–1187.

[7] [7] C. Di Perna. F. Stazi, A. Ursini Casalena, M. D'Orazio. Influence of the internal inertia of the building envelope on summertime comfort in buildings with high internal heat loads. Energy and Buildings 43 (2011) 200-206.

[8] N. Aste, A. Angelotti, M. Buzzetti. The influence of the external walls thermal inertia on the energy performance of well insulated buildings. Energy and Buildings 41 (2009) 1181-1187.

[9] D.E.M. Bond, W.W. Clark, M. Kimber. Configuring wall layers for improved insulation performance. Applied Energy 112 (2013) 235–245.

[10] C. Baglivo, P.M. Congedo. Design method of high performance precast external walls for warm climate by multi-objective optimization analysis, Energy 90 (2015) 1645-1661.[11] C. Baglivo, P.M. Congedo, A. Fazio, D. Laforgia. Multi-objective optimization analysis for high efficiency external walls of zero energy buildings (ZEB) in the Mediterranean climate. Energy and Buildings 84 (2014) 483-492.

[12] V. Sambou, B. Lartigue, F. Monchoux, M. Adj. Thermal optimization of multilayered walls using genetic algorithms. Energy and Buildings 41 (2009) 1031-1036.

[13] I. Zacà, D. D'Agostino, P.M. Congedo, C. Baglivo, Assessment of cost-optimality and technical solutions in high performance multi-residential buildings in the Mediterranean area. Energy and Buildings 102 (2015) 250-265.

[14] Directive 2009/28/EC on the promotion of the use of energy from renewable sources.

[15] International Energy Agency. Technology Roadmap. Energy-efficient Buildings: Heating and Cooling Equipment 2011

[16] C. Aprea, R. Mastrullo, C. Renno. Experimental analysis of the scroll compressor performances varying its speed. Applied Thermal Engineering 26 (2006) 983-992.

[17] D.B. Crawley, J.W. Hand, M. Kummert, B.T. Griffith. Contrasting the capabilities of building energy performance simulation programs. Building and Environment 43 (2008) 661–673.

[18] S. de Wit. Uncertainty in building simulation, in: A. Malkawi, G. Augen-broe (Eds.), Advanced Building Simulation, Taylor & Francis, Abingdon (UK), 2004.

[19] F. Domínguez-Muñoz, B. Anderson, J.M. Cejudo-López, A. Carrillo-Andrés, Uncertainty in the thermal conductivity of insulation materials, Energy and Buildings 42 (11) (2010) 2159–2168.

[20] P.G. Cesaratto, M. De Carli. A measuring campaign of thermal conductance in situ and possible impacts on net energy demand in buildings. Energy and Buildings 59 (2013) 29–36.

[21] A. Byrne, G. Byrne, A. Davies, A.J. Robinson. Transient and quasi-steady thermal behaviour of a building envelope due to retrofitted cavity wall and ceiling insulation, Energy and Buildings 61 (2013) 356–365.

[22] B.R. Anderson. Site-Testing Thermal Performance: a CIB survey. Batiment International, Building Research and Practice 12 (1984) 147–149.

[23] J.B. Siviour. Experimental U-values of some house walls. Building Services Engineering Research and Technology 15 (1) (1994) 35–36.

[24] C. Rye, U-Value Report (The SPAB research report 1). London (UK): The Society for the Protection of Ancient Buildings (SPAB), 2012.

[25] L. Schibuola, M. Scarpa. On-field validation of a seasonal performance calculation method for chillers in buildings. Energy Conversion and Management 85 (2014) 62-69.

[26] A. de Gracia, A. Castell, M. Medrano, L.F. Cabeza. Dynamic thermal performance of alveolar brick construction System. Energy Conversion and Management 52 (2011) 2495–2500.

[27] P. Riviere et al. Ecodesign lot 10 Study on ventilation (2009). http://www.eceee.org/ecodesign/products/airco_ventilation (accessed June 2015)